Electronic Supplementary Material (ESI) for Organic & Biomolecular Chemistry.
This journal is © The Royal Society of Chemistry 2018

Supporting Information

Tetracyclic Pyrazine-fused Furazans as Insensitive Energetic Materials: Syntheses, Structures, and Properties

Table of Contents

1. General methods
2. X-ray crystallography details
3. IR spectra
4. TG plots
5. MS, ^{1}H and ^{13}CNMR spectra
6. Theoretical calculations
7. Electrostatic potential surfaces and HOMO and LUMO energy levels of **2** and **3**.
8. Performance of compound **4**

General methods

All reagents were purchased from Energy Chemical of analytical grade and were used as supplied, if not stated otherwise. ^{1}H, ^{13}C spectra were recorded using a 500 MHz (Bruker AVANCE III 500) nuclear magnetic resonance spectrometer operating at 500 and 50.69 MHz, respectively. Chemical shifts in the ^{1}H and ^{13}C spectra are reported relative to Me_4Si as external standards. The melting and decomposition (onset) points were obtained on a differential scanning calorimeter (Mettler Toledo DSC823e) at a scan rate of 5 °C min^{-1} in closed Al containers with a nitrogen flow of 50 ml min^{-1}. IR spectra were recorded using KBr pellets for solids on a Thermo Nicolet iS10 spectrometer. Elemental analyses were carried out on a vario EL III CHNOS elemental analyzer.

X-ray Crystallography detail

A colorless block crystal (**2**) of dimensions 0.14×0.13×0.10 mm^3, a colorless block crystal (**3**) of dimensions 0.13×0.12×0.08 mm^3, and a colorless sheet crystal (**4**) of dimensions 0.27×0.16×0.04 mm^3 were mounted on an Enraf-Nonius CAD4 four-circle diffractometer using graphite-monochromated Mo Ka radiation (λ = 0.71073 Å) at 173 K. Corrections for Lorentz and polarization effects and for absorption (ψ scan) were applied. The structure was solved by direct methods using SHELXS-97 and refined by full-matrix least-squares calculation on F^2 with SHELXL-97. All non-hydrogen atoms were refined anisotropically. All hydrogens were placed in calculated positions and were assigned fixed isotropic thermal parameters at 1.2 times the equivalent isotropic U of the atoms to which they were attached and allowed to ride on their respective parent atoms. The contributions of these hydrogen atoms were included in the structure-factor calculations.

Table S1 Crystallographic data for **2**, **3**, and 3(**4**).$2H_2O$.

Compound	**2**	**3**	3(**4**).$2H_2O$
Formula	$C_6H_6N_8O_2$	$C_6H_2N_8O_2$	$3(C_4H_2N_4O_3).2H_2O$
M_w	222.19	218.16	498.32
Crystal system	Orthorhombic	Monoclinic	Monoclinic
Space group	Pbca	P21/n	P21/c
a [Å]	8.0308(12)	5.7793(6)	19.2788(12)
b [Å]	7.8229(10)	11.6585(15)	5.4732(4)
c [Å]	12.8172(18)	5.7805(6)	19.4681(13)
α[°]	90	90	90
β[°]	90	100.280(4)	111.922(2)
γ[°]	90	90	90
V [$Å^3$]	805.23(19)	383.23(7)	1905.7(2)
Z	4	2	4
T [K]	174	173	173
λ [Å]	0.71073	0.71073	0.71073
ρ_{calcd}[g cm^{-3}]	1.833	1.891	1.737
μ [mm^{-1}]	0.146	0.152	0.155
F(000)	456	220	1016.0
θ range[°]	3.18-25.34	4.59-24.64	3.42-25.31
Index ranges	$-6 \le h \le 9$	$-6 \le h \le 6$	$-23 \le h \le 22$
	$-9 \le k \le 9$	$-14 \le k \le 14$	$-5 \le k \le 6$
	$-15 \le l \le 15$	$-6 \le l \le 6$	$-23 \le l \le 23$
Data/restraints/ parameters	738/0/79	688/0/76	3483/364/30
GOF on F2	1.043	1.056	1.054
$R[F^2 > 2\sigma(F^2)]$	0.0485	0.0448	0.0468
$wR(F^2)$	0.1114	0.0988	0.0985

Table S2 Bond lengths (Å) and bond angles (°) for **2**.

C1 N2 1.429(4)	C2 N2 1.352(3)	N1 H1A 0.86(3)
C1 N1 1.476(3)	C2 C3 1.433(4)	N2 H2A 0.84(3)
C1 C1 1.552(5)	C3 N3 1.298(4)	N3 O1 1.408(4)
C1 H1 1.0000	C3 N1 1.367(4)	N4 O1 1.414(3)
C2 N4 1.293(4)	N1 C3 1.367(4)	
N2 C1 N1 111.6(2)	N4 C2 C3 110.7(3)	C1 N1 H1A 118(2)
N2 C1 C1 110.8(3)	N2 C2 C3 121.4(3)	C2 N2 C1 118.2(2)
N1 C1 C1 108.00(18)	N3 C3 N1 129.1(3)	C2 N2 H2A 119(2)
N2 C1 H1 108.8	N3 C3 C2 109.8(3)	C1 N2 H2A 119(2)
N1 C1 H1 108.8	N1 C3 C2 121.1(2)	C3 N3 O1 104.3(3)
C1 C1 H1 108.8	C3 N1 C1 112.1(2)	C2 N4 O1 103.8(3)
N4 C2 N2 127.8(3)	C3 N1 H1A 114.3(19)	N3 O1 N4 111.3(2)

Table S3 Bond lengths (Å) and bond angles (°) for **3**.

C1 N2 1.302(3)	C2 N4 1.372(3)	N1 C3 1.343(4)
C1 N1 1.369(3)	C3 N4 1.315(3)	N1 H1 0.86(3)
C1 C2 1.412(4)	C3 N1 1.343(4)	N2 O1 1.410(3)
C2 N3 1.306(3)	C3 C3 1.507(5)	N3 O1 1.397(3)
N2 C1 N1 128.7(2)	N4 C3 N1 118.5(2)	C1 N1 H1 121.7(19)
N2 C1 C2 111.1(2)	N4 C3 C3 123.4(3)	C1 N2 O1 103.3(2)
N1 C1 C2 120.2(2)	N1 C3 C3 118.1(3)	C2 N3 O1 104.2(2)
N3 C2 N4 126.3(2)	C3 N1 C1 119.1(2)	C3 N4 C2 115.3(2)
N3 C2 C1 109.8(2)	C3 N1 H1 119.1(19)	N3 O1 N2 111.63(18)
N4 C2 C1 123.9(2)		

Table S4 Bond lengths (Å) and bond angles (°) for 3(**4**)·2H_2O.

C1A N2A 1.295(3)	C3B N3B 1.358(3)	N2A O1A 1.405(3)
C1A N4A 1.368(3)	C3B C4B 1.543(3)	N3A H3AA 0.852(17)
C1A C2A 1.413(3)	C4B O3B 1.218(3)	N4A H4AA 0.858(16)
C2A N1A 1.291(3)	C4B N4B 1.358(3)	N1B O1B 1.407(3)
C2A N3A 1.377(3)	C1C N2C 1.300(3)	N2B O1B 1.406(3)
C3A O2A 1.227(3)	C1C N4C 1.368(3)	N3B H3BA 0.867(16)
C3A N3A 1.344(3)	C1C C2C 1.408(3)	N4B H4BA 0.854(17)
C3A C4A 1.539(3)	C2C N1C 1.293(3)	N1C O1C 1.397(3)
C4A O3A 1.218(3)	C2C N3C 1.379(3)	N2C O1C 1.407(3)
C4A N4A 1.362(3)	C3C O2C 1.222(3)	N3C H3CA 0.857(16)
C1B N2B 1.301(3)	C3C N3C 1.352(3)	N4C H4CA 0.865(17)
C1B N4B 1.368(3)	C3C C4C 1.542(3)	O4 H4A 0.867(17)
C1B C2B 1.416(3)	C4C O3C 1.219(3)	O4 H4B 0.855(18)
C2B N1B 1.294(3)	C4C N4C 1.351(3)	O5 H5A 0.829(19)
C2B N3B 1.369(3)	N1A O1A 1.404(3)	O5 H5B 0.83(2)

C3B O2B 1.214(3)	O5' H5D 0.82(2)	O5' H5C 0.82(2)
N2A C1A N4A 128.7(2)	O2B C3B N3B 123.6(2)	C1A N2A O1A 103.5(2)
N2A C1A C2A 110.5(2)	O2B C3B C4B 117.9(2)	C3A N3A C2A 120.1(2)
N4A C1A C2A 120.9(2)	N3B C3B C4B 118.4(2)	C3A N3A H3AA 122.3(19)
N1A C2A N3A 127.5(2)	O3B C4B N4B 123.6(2)	C2A N3A H3AA 117.6(18)
N1A C2A C1A 110.8(2)	O3B C4B C3B 117.7(2)	C4A N4A C1A 120.0(2)
N3A C2A C1A 121.7(2)	N4B C4B C3B 118.7(2)	C4A N4A H4AA 118.7(18)
O2A C3A N3A 123.9(2)	N2C C1C N4C 127.8(2)	C1A N4A H4AA 121.3(18)
O2A C3A C4A 117.6(2)	N2C C1C C2C 110.3(2)	C2B N1B O1B 104.11(19)
N3A C3A C4A 118.5(2)	N4C C1C C2C 121.9(2)	C1B N2B O1B 104.00(19)
O3A C4A N4A 122.4(2)	N1C C2C N3C 128.1(2)	C3B N3B C2B 120.3(2)
O3A C4A C3A 118.8(2)	N1C C2C C1C 110.9(2)	C3B N3B H3BA 118.8(17)
N4A C4A C3A 118.8(2)	N3C C2C C1C 121.0(2)	C2B N3B H3BA 120.5(17)
N2B C1B N4B 127.9(2)	O2C C3C N3C 124.0(2)	C4B N4B C1B 119.7(2)
N2B C1B C2B 110.2(2)	O2C C3C C4C 117.7(2)	C4B N4B H4BA 118.8(18)
N4B C1B C2B 121.9(2)	N3C C3C C4C 118.3(2)	C1B N4B H4BA 121.2(18)
N1B C2B N3B 128.6(2)	O3C C4C N4C 123.0(2)	C2C N1C O1C 103.6(2)
N1B C2B C1B 110.5(2)	O3C C4C C3C 117.9(2)	C1C N2C O1C 103.4(2)
N3B C2B C1B 120.9(2)	N4C C4C C3C 119.2(2)	C3C N3C C2C 120.1(2)
N2B O1B N1B 111.14(17)	C2A N1A O1A 103.5(2)	C3C N3C H3CA 122.4(18)
N1C O1C N2C 111.79(18)	H4A O4 H4B 102(3)	C2C N3C H3CA 117.3(19)
H5A O5 H5B 106(3)	N1A O1A N2A 111.65(18)	C4C N4C C1C 119.5(2)
H5C O5' H5D 108(4)	C1C N4C H4CA 120.3(18)	C4C N4C H4CA 120.1(19)

IR Spectra

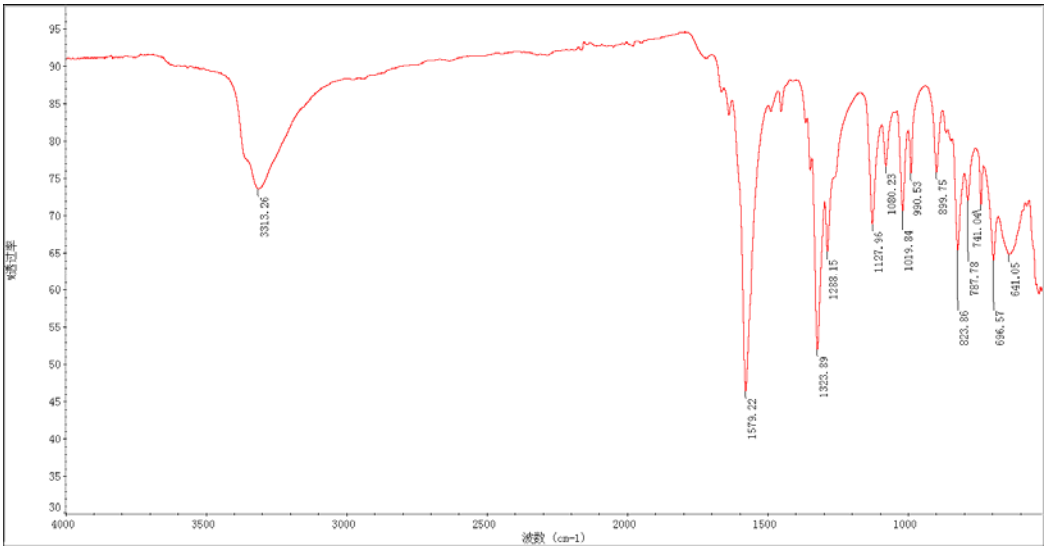

Figure S1 IR spectra for **2**.

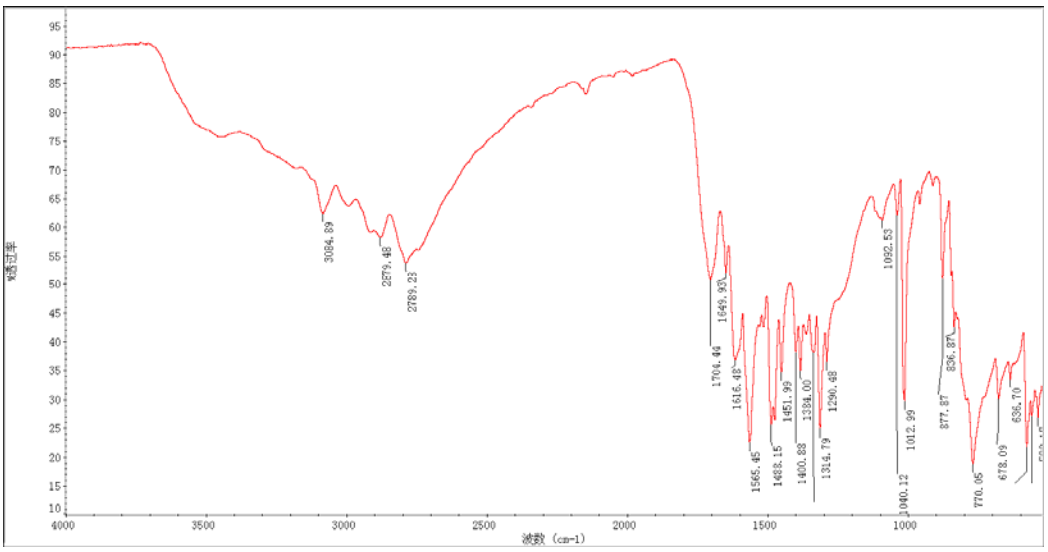

Figure S2 IR spectra for **3**.

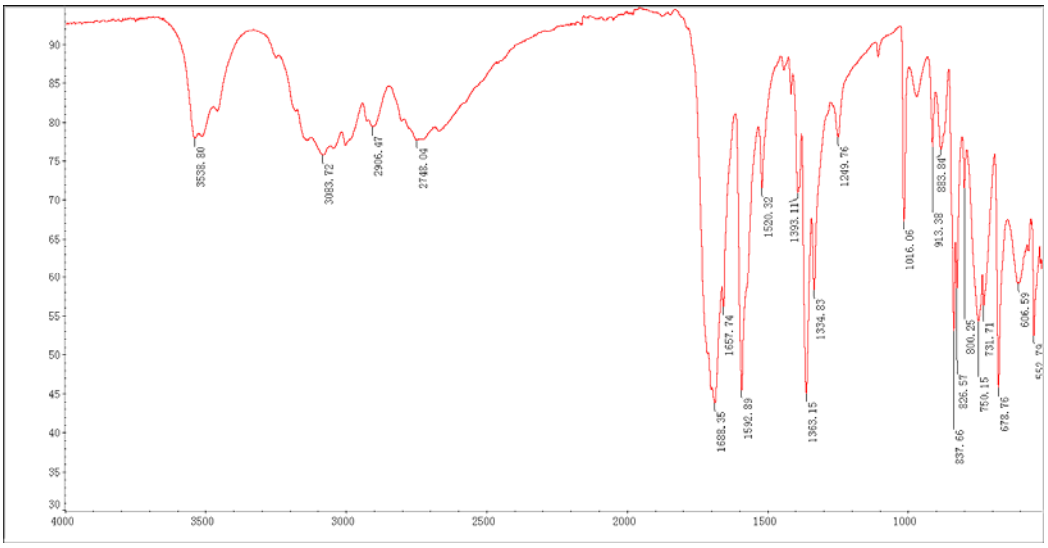

Figure S3 IR spectra for **4**.

TG plots

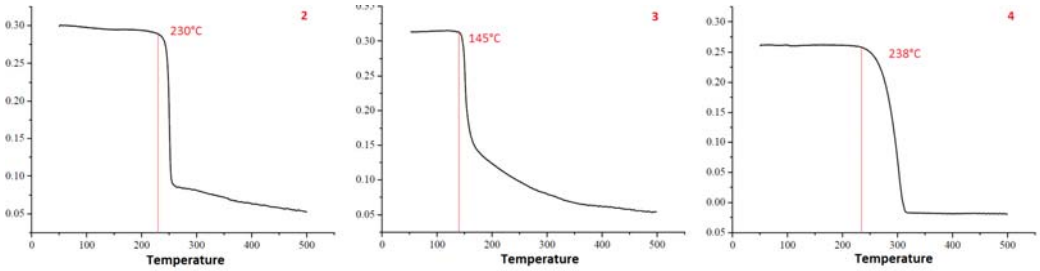

Figure S4 TG plots for compounds **2**, **3**, and **4**.

MS, ^{1}H and ^{13}CNMR spectra

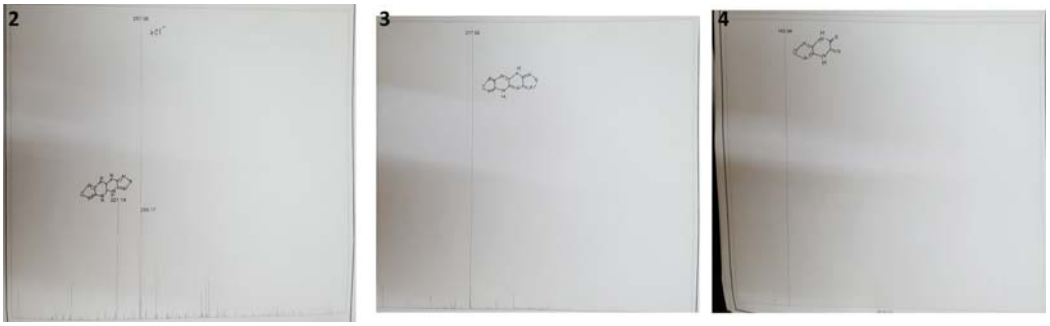

Figure S5 MS spectra for compounds **2**, **3**, and **4**.

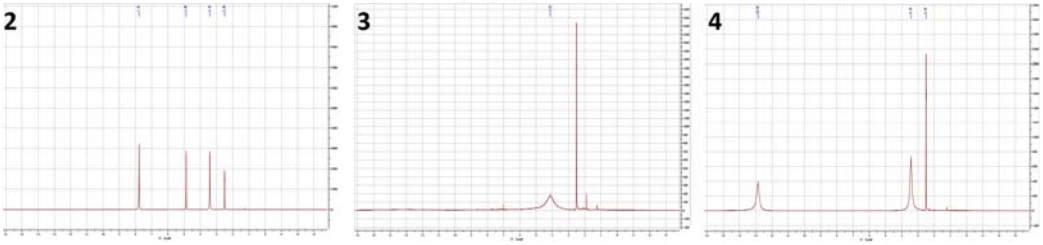

Figure S6 ^{1}HNMR spectra for compounds **2**, **3**, and **4**.

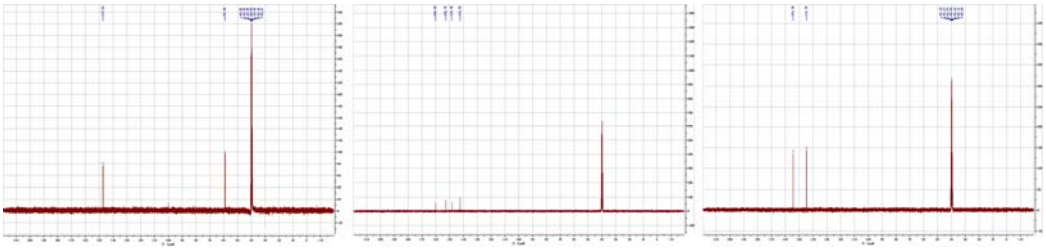

Figure S7 ^{13}CNMR spectra for compounds **2**, **3**, and **4**.

Theoretical calculation

All of the ab initio calculations involved in this work were carried out using the Gaussian 09 suite of programs. The geometric optimization and frequency analyses of the structures are based on available single-crystal structures and using the B3LYP functional with the 6-31++G(d,p) basis set. The geometrical were optimized with no constraints imposed under default convergence criteria. Total energy (E_0) and zero-point energy (ZPE) were calculated with vibrational frequency analysis. The heats of formation were obtained by using the isodesmic reaction approach. Atomization energies were obtained by employing the G2 ab initio method. All of the optimized structures were characterized to be true local energy minima on the potential energy surface without imaginary frequencies.

NIC plots of gradient isosurfaces (s = 0.5 au) for **2** and **3** unit cells. The geometries of the unit cells were listed from crystal data. The calculations were carried out using the Gaussian 09 suite of programs. The pictures of the noncovalent interactions were drawn by VMD 1.9.3 program. The surfaces are colored on a blue-green-red scale indicating strong attractive interactions, weak attractive, and strong nonbonded overlap, respectively.

Electrostatic potential surfaces and HOMO and LUMO energy levels

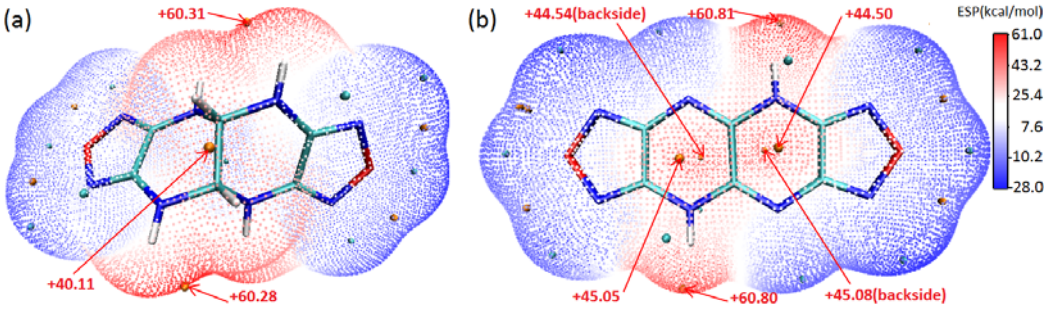

Figure S5 Electrostatic potential surfaces of **2** and **3**. The minimum and maximum ESP are marked with blue and orange points, respectively.

As shown in Figure S5, it is clear that compound **3** possesses higher maximum electrostatic surface potentials than compound **2** in the similar places, which indicates compound **3** shows worse stability than compound **2**.

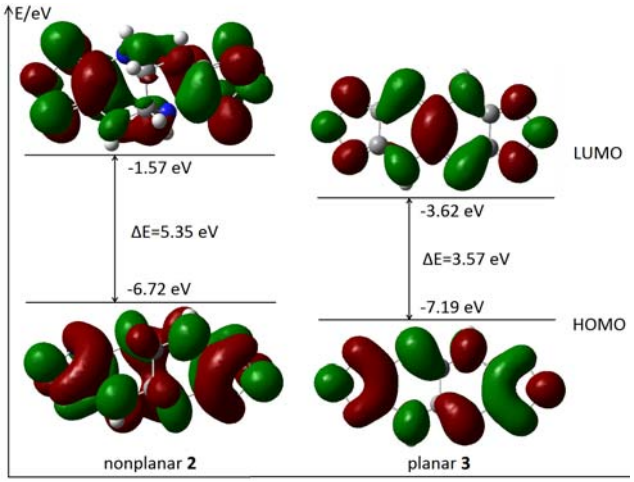

Figure S6 HOMO and LUMO energy levels and energy gaps of compounds **2** and 3.

As shown in Figure S6, the energy gap of compound **3** is smaller than that of compound **2**, which means compound **3** is less stable than compound **2**.

Performance of compound 4

Table S5. Physiochemical properties and detonation parameters of **4**.

Compd	T_d[a]	d[b]	ΔH_f[c]	D[d]	P[e]	IS[f]	FS[g]
	[°C]	[g cm^{-3}]	[kJ mol^{-1}]	[m s^{-1}]	[GPa]	[J]	[N]
4	238	1.70	-46.2	7319	22.9	>40	>360

[a] Thermal decomposition temperature (DSC, onset, 5 °C min^{-1}). [b] Density measured by gas pycnometer. [c] Calculated heats of formation (Gaussian 09[10]). [d] Detonation velocity (K-J equation[11]). [e] Detonation pressure (K-J equation). [f] Impact sensitivity. [g] Friction sensitivity. [h] Ref 7c.